

Processing of glass-ceramics in the $\text{SiO}_2\text{--Al}_2\text{O}_3\text{--B}_2\text{O}_3\text{--MgO--CaO--Na}_2\text{O--(P}_2\text{O}_5\text{)--F}$ system via sintering and crystallization of glass powder compacts

D.U. Tulyaganov, S. Agathopoulos, H.R. Fernandes, J.M.F. Ferreira *

Department of Ceramics and Glass Engineering, University of Aveiro, CICECO, 3810-193 Aveiro, Portugal

Received 3 January 2005; received in revised form 20 January 2005; accepted 12 February 2005

Available online 10 May 2005

Abstract

Glass-ceramics were produced by crystallization of glasses in the $\text{SiO}_2\text{--Al}_2\text{O}_3\text{--B}_2\text{O}_3\text{--MgO--CaO--Na}_2\text{O--F}$ system. The experimental results showed that bulk glasses are prone to surface crystallization. Hence, crystallization of bulk glasses resulted in non-homogeneous crystalline materials, which comprised relatively coarse crystals. Therefore, processing was realized using glass-powder compacts. Maximum densification was reached at 700–750 °C. This interval is positioned at relatively lower temperatures than those often reported for similar sintered glass-ceramics. Doping with P_2O_5 improved sintering behaviour and broadened sintering temperature range. Sintering between 750 and 800 °C resulted in materials, which exhibited dense crystalline microstructure and the maximum flexural strength.

© 2005 Elsevier Ltd and Techna Group S.r.l. All rights reserved.

Keywords: A. Sintering; B. Microstructure-final; D. Glass-ceramics; Crystallization

1. Introduction

The production of alkaline-earth aluminosilicate glasses in the system $\text{SiO}_2\text{--Al}_2\text{O}_3\text{--MgO--CaO}$ has been broadly investigated in the past decade. Crystalline phases, such as cordierite, diopside, wollastonite, melilite, etc., have been precipitated from glasses under controlled conditions resulting in glass-ceramics with attractive dielectric properties and high mechanical and chemical resistance [1–8].

Special nucleation agents can stimulate external nucleation whereby micro-heterogeneities are developed and crystallization can subsequently begin. The process advances by the transformation of the amorphous reservoir of the parent glass into uniform microcrystalline ceramic [4,8].

Sintering of glass-powder compacts is an alternative processing route of producing fully dense glass-ceramics [1,4–6]. Glass powders with high specific surface area

intrinsically provide uniformly scattered nucleus sites throughout the entire volume of the glass. Thus no addition of special nucleating agents is required. In this processing route, sintering must preferably take place prior to crystallization. Chemical composition, particle size, and heat treatment parameters are few of the factors which can cause a shift of crystallization to higher temperatures [1,9]. In general, reduction of glass-viscosity, which in other words corresponds to increasing driving force of densification, can benefit sintering process and shift the occurrence of crystallization at higher temperatures. In multi-component systems, the excess of free energy related to the chemical gradients can generally improve diffusion process and enhance sintering [1,10].

In this work, glass-ceramics with uniform crystalline microstructure were produced from the multi-component $\text{SiO}_2\text{--Al}_2\text{O}_3\text{--B}_2\text{O}_3\text{--MgO--CaO--Na}_2\text{O--(P}_2\text{O}_5\text{)--F}$ system. In particular, two glass compositions were investigated. The basic glass composition, designated hereafter as A, had a formula of $4.54\text{Na}_2\text{O} \cdot 13.64\text{MgO} \cdot 31.82\text{CaO} \cdot 1.14\text{Al}_2\text{O}_3 \cdot 3.41\text{B}_2\text{O}_3 \cdot 40.91\text{SiO}_2 \cdot 4.54\text{CaF}_2$. A modified composi-

* Corresponding author. Tel.: +351 234 370242; fax: +351 234 425300.
E-mail address: jmf@cv.ua.pt (J.M.F. Ferreira).

tion, designated as A-P, derived from A by doping with P_2O_5 and had a composition of $4.48Na_2O \cdot 13.45MgO \cdot 31.40CaO \cdot 1.12Al_2O_3 \cdot 3.36B_2O_3 \cdot 40.36SiO_2 \cdot 3.36B_2O_3 \cdot 40.36SiO_2 \cdot 4.48CaF_2 \cdot 1.35P_2O_5$.

Glasses in both bulk and powder-compact forms were subjected to heat treatment. This work has addressed its main focus at the processing of glass-ceramics via sintering and crystallization of glass-powder compacts which, according to the presenting results, can be considered as a favourable production route of materials with desirable microstructure and properties in the investigated multi-component system.

2. Materials and experimental procedure

The chemical compositions of the glasses A and A-P (in wt.%) are presented in Table 1. Powders of technical grade of silicon oxide (purity >99.5%), aluminium oxide (>99.5%), and calcium carbonate (>99.5%), and reactive grade of H_3BO_3 , $4MgCO_3 \cdot Mg(OH)_2 \cdot 5H_2O$, Na_2CO_3 , CaF_2 and $NH_4H_2PO_4$, were used. Homogeneous mixtures of batches (~100 g), obtained by ball milling, were preheated at 1000 °C for 1 h for decarbonization and then melted in corundum crucibles at 1400 °C for 1 h, in air.

Glasses in bulk form were produced by casting of melts on preheated bronze moulds and annealing at 600 °C. Heat treatment of bulk glasses was carried out at 700, 800 and 900 °C for 1 h (heating rate 5 K/min). To study the thermal behaviour of the glasses, differential thermal analysis (DTA, Labsys Setaram TG-DTA/DSC, France, up to 1000 °C, heating rate 5 K/min, in air) and dilatometry (Bahr Thermo Analyse DIL 801 L, Germany, up to 800 °C, heating rate 3 K/min) were carried out.

Frit glass powders were obtained by quenching of glass melts in cold water. The frits were dried and then milled in a high-speed porcelain mill, resulting in powders with mean particle sizes of 13.7 and 17.6 μm for A and A-P, respectively (measured by Coulter LS 230, UK; Fraunhofer optical model). The glass frit powders were granulated by mixing with a 5 vol.% polyvinyl alcohol solution (PVA) in a proportion of 97.5 wt.% of frit and 2.5 wt.% of PVA. Rectangular bars with dimensions of 4 mm \times 5 mm \times 50 mm were prepared by uniaxial pressing (80 MPa). After debinding at 450 °C for 2 h, the bars were sintered at several temperatures between 650 and 920 °C for 1 h at a slow heating rate of 2–3 K/min to avoid deformation.

The following techniques were also used to characterize the produced materials. The crystalline phases formed were

detected by X-ray diffraction analysis (XRD, Rigaku Geigerflex D/Mac, C Series, Cu $K\alpha$ radiation, Japan). Microstructure observations and chemical analyses at polished and then etched glass and glass-ceramic surfaces (immersion in 2 vol.% HF solution for 45 s and 4 min, respectively) were done by scanning electron microscopy (SEM, Hitachi S-4100, Japan, 25 kV acceleration voltage) and energy dispersive spectroscopy (EDS). Archimedes method (i.e. immersion in ethylenoglycol) was employed to measure the apparent density of glass and glass-ceramic blocks. Vickers microhardness was estimated from ten indentations for each sample (Shimadzu microhardness tester type M, Japan, load of 9.8 N). Flexural strength (three-point bending) was measured with parallelepiped bars (3 mm \times 4 mm \times 40 mm) (Shimadzu Autograph AG 25 TA, 0.5 mm/min displacement; the presenting results are the average of 12 bars). Water absorption was measured according to the ISO standard 10545-3, 1995. The linear shrinkage during sintering was calculated from the dimensions of the green and the sintered samples.

3. Results and discussion

From dilatometry (plots are not shown), the transition temperature (T_g) of both the glasses A and A-P was recorded at ~625 °C. The softening points were at ~670 °C for A and at slightly lower temperature (~665 °C) for A-P.

SEM observations of the annealed bulk glasses revealed no striking differences between the microstructures of the two investigated glasses, whereas both of them featured clear evidence of liquid–liquid phase separation (Fig. 1a). After heat treatment at 700 °C, the effect of phase separation was more pronounced but there was no evidence of crystallization yet (image is not shown). The bulk glasses were prone to surface crystallization over heat treatment at 800 °C (Fig. 1b). The onset of crystal growth advances from the surface to the core after heat treatment at 900 °C. However, crystals of different morphology were observed at the regions close to the surface (Fig. 1c) and in the core of the bulk samples (Fig. 1d). In particular, coarse columnar and dendritic crystals, marked with 1 and 2, respectively, in Fig. 1c, dominated near the surface, whereas dendritic crystal 2 together with fibrous crystals, marked with 3 in Fig. 1d, were observed in the core of the samples. According to the chemical analysis (by EDS), the crystal 1, whose composition (in wt.%) was 48.8–49.8 SiO_2 , 11.7–12.0 Al_2O_3 , 17.4–20.8 MgO , 15.9–20.1 CaO and 1.0–2.5 Na_2O , can be assigned to aluminous pyroxenes, assuming a slight deviation from their stoichiometry [11].

According to the literature, partial substitution of Ca-Tschermak's ($CaAl_2SiO_6$) components for diopside is possible. Omar et al. [12] have reported that complex pyroxene containing up to 48% of $CaAl_2SiO_6$ can be obtained by crystallization under non-equilibrium conditions. In the course of investigations of glasses based on the

Table 1
Chemical composition of the investigated glasses (wt.%)

Glass	SiO_2	Al_2O_3	B_2O_3	CaO	MgO	P_2O_5	Na_2O	CaF_2
A	42.51	2.00	4.10	30.86	9.51	–	4.87	6.14
A-P	41.13	1.94	3.97	29.86	9.20	3.24	4.72	5.94

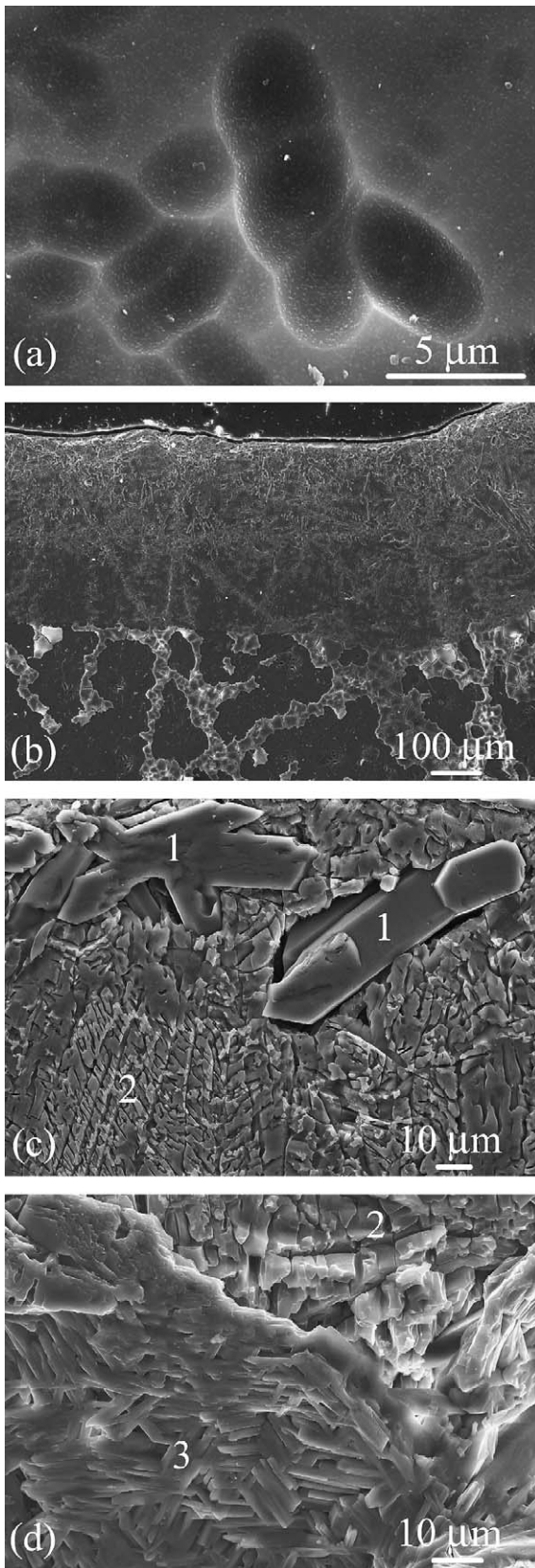


Fig. 1. Microstructure of the annealed bulk glass A (a), and its evolution after 1 h of heat treatment at 800 °C (b) (the outer surface of the sample is at the top side of the image), and at 900 °C at a region close to the outer surface (c) and at the core of the bulk sample (d). The images, obtained by SEM

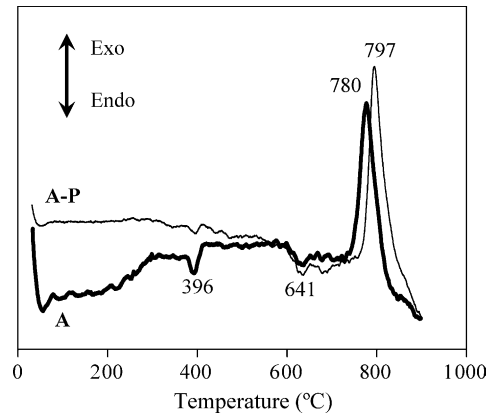


Fig. 2. DTA of frit powders of the glasses A and A-P, granulated by mixing in a 5 vol.% PVA.

diopside-Ca-Tschermak's-fluorapatite system, Salama et al. [13] have found that the higher limit of isomorphous substitution of $\text{CaAl}_2\text{SiO}_6$ accommodated in diopside structure is 25%. Substitution beyond this limit causes also formation of gehlenite ($\text{Ca}_2\text{Al}_2\text{SiO}_7$).

The crystals 2 and 3 (Fig. 1c and d) had similar chemical composition (by EDS) laying in the range of 42.7–43.5 SiO_2 , 9.4–9.5 Al_2O_3 , 8.5–9.5 MgO , 33.4–34.4 CaO and 4.2–5.0 Na_2O (wt.%). Considering that Na can substitute Ca in melilite, these crystals can be assigned to solid solutions of akermanite and gehlenite with a general formula of $\text{CaO} \cdot (1-x)\text{MgO} \cdot x\text{Al}_2\text{O}_3 \cdot (2-x)\text{SiO}_2$. Note that the use of corundum crucibles should have inevitably caused an Al_2O_3 uptake. Chang et al. [14] have experimentally found that the amount of Al_2O_3 introduced from the alumina crucibles to the melt during preparation of the apatite-wollastonite glass-ceramics was slightly higher than 1 wt.%.

Consequently, the crystallization of the samples of bulk glasses exhibited features of surface crystallization while the microstructure of the resultant glass-ceramics was non-homogeneous and comprised relatively coarse crystals. These results justify the shift of our interest to the processing of glass-ceramics via glass-powder compacts.

In this processing route, the correct set up of sintering and crystallization schedules, as it has been described above (Section 2), was done with the aid of DTA analysis of similarly treated glass-powders (i.e. granulation by mixing in a 5 vol.% PVA). The DTA curves (Fig. 2) showed small endothermic peaks at ~ 400 °C, assigned to the decomposition of PVA, and at ~ 640 °C, attributed to the glass-transition temperature, following by a single, strong and symmetric exothermic crystallization peak, with maxima at 780 and 797 °C for A and A-P, respectively.

Fig. 3 shows the influence of sintering temperature on the density and the linear shrinkage of the two investigated compositions. For comparison purposes, it is mentioned that

using secondary electron mode, correspond to polished surfaces after etching of with 2% HF solution.

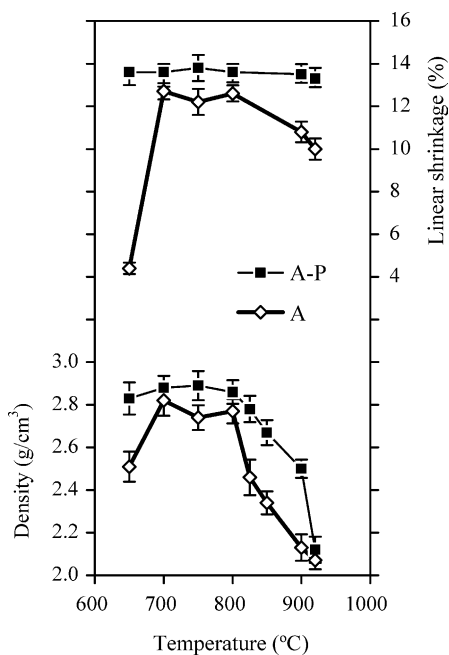


Fig. 3. Density and linear shrinkage of glass-powder compacts of A and A-P compositions sintered at different temperatures.

the apparent density of the bulk glasses was measured as 2.80 g/cm^3 for both A and A-P. According to the plots of Fig. 3, glass-powder compacts reached a maximum of densification in the range of $700\text{--}750^\circ\text{C}$. This interval is positioned at certainly lower temperatures than the sintering temperatures reported for similar glass-ceramics [1,4,11]. The early densification should be due to the presence of B_2O_3 , Na_2O and CaF_2 . Earlier studies have shown that these compounds can improve sintering ability of glass powders since they act as fluxes and thus they increase liquid fluidity of viscous flow [11,15,16].

The plots of Fig. 3 clearly show that the modified A-P composition features a superior sintering behaviour comparing to composition A, because sintering starts at lower temperatures and densification is always higher, reaching a maximum of density (2.89 g/cm^3) and shrinkage (13.8%) at 750°C , which safely occurs at higher temperatures (especially the linear shrinkage).

The differences between the curves of A and A-P in Fig. 3 might indicate that P_2O_5 has an influence on diffusion process. Earlier studies have reported that small additions of several oxides, such as P_2O_5 , to certain glasses can impart excellent sinterability [16,17]. Our experimental results show that P_2O_5 has probably increased the stability of the glass against crystallization at the temperatures of sintering onset. Similarly, in the case of sodium aluminium phosphate glasses, B_2O_3 has been reported as a very effective compound for improving stability of glasses and for suppressing crystallization [18].

The evolution of the phases over increasing sintering temperature is shown in Fig. 4. At 650°C , both materials are still amorphous. Increasing temperature caused a gradual

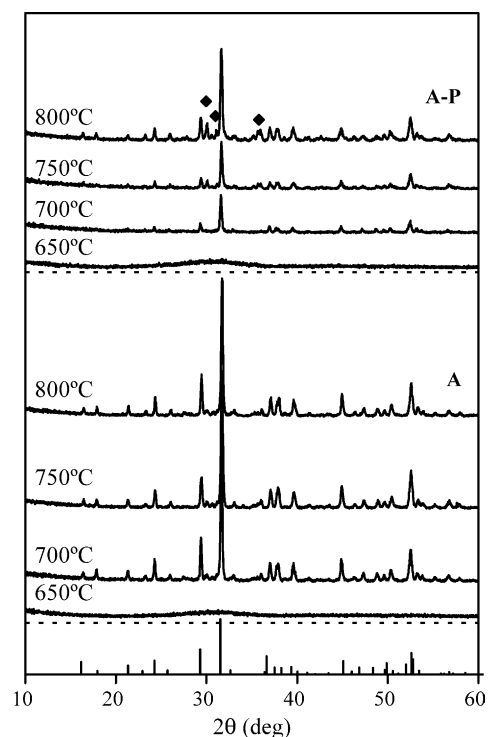


Fig. 4. Phase evolution over increasing crystallization temperature of A and A-P glass-powder compacts (JCPDS cards: akermanite, $\text{Ca}_2\text{MgSi}_2\text{O}_7$, 87-0052—it is plotted at the bottom side of the plot; diopside, $\text{CaMgSi}_2\text{O}_6$, 75-1577—it is denoted with (◆); the intensities of the original spectra have not been normalized).

devitrification in both A and the P_2O_5 -doped A-P glasses. Akermanite predominantly precipitated at $\geq 700^\circ\text{C}$, while weak peaks of diopside ($\text{CaMgSi}_2\text{O}_6$) were detected at 750°C and at 800°C , slightly stronger in A-P. The presence of a single exothermic peak in the DTA plots (Fig. 2) agrees fairly well with the crystallization of one predominant phase (Fig. 4). Nevertheless, Fig. 4 shows that akermanite has been already formed at 700°C , while Fig. 2 has registered the maximum of the crystallization peaks at considerably higher temperatures. This difference should be attributed to the influence of heating rate. It is known that the evolution of crystalline phases occurs at lower temperatures in the case lower heating rates [19]. In this work, the heating rate of DTA was 5 K/min and of sintering $2\text{--}3 \text{ K/min}$. However, the crystallization onset obviously occurs at lower temperatures than the maximum of the crystallization peak (Fig. 2).

The glass-ceramics of composition A crystallized at 800°C for 1 h exhibited a dense crystalline microstructure. In general, a network of small ($1\text{--}2 \mu\text{m}$) interlocking elongated and prismatic crystals of akermanite embedded in a glassy phase was observed (Fig. 5a). Assemblages of well-oriented very fine crystals ($\sim 1 \mu\text{m}$) were observed at other places of the glass-ceramics (inset of Fig. 5a). The similarly heat-treated glass-ceramic of A-P composition exhibited similar microstructure, but the glassy phase seems to be more abundant (Fig. 5b). Fig. 5b shows at the same image the two configurations described for the glass-ceramics A (Fig. 5a).

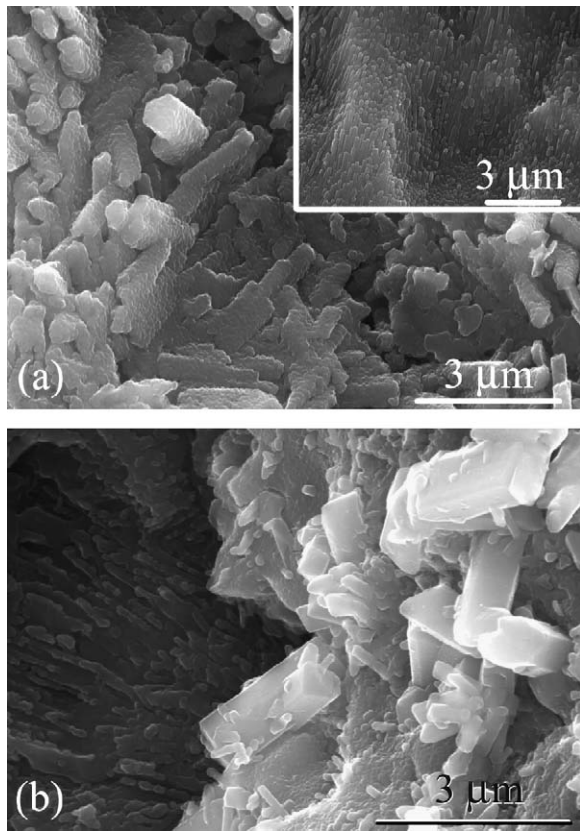


Fig. 5. Characteristic microstructures of glass-ceramics A (a) and A-P (b) made of glass-powder compacts heat-treated at 800 °C for 1 h, observed by SEM using secondary electron mode after etching of polished surfaces with 2% HF solution.

In glass-ceramics, the desired order of events generally presumes that sintering stage should end before the beginning of intensive crystallization. In such a case, the resultant glass-ceramic will feature highly dense structure with low porosity. In this investigation, both glass compositions have seemingly served this purpose. The presence of P_2O_5 in the A-P composition further improved sintering behaviour (Fig. 3).

Nevertheless, when densification has been almost completed then secondary porosity often appears likely due to the crystallization of phases, which are denser than the parent glass. For instance, the densities of akermanite and of the glass whose chemical composition corresponds to akermanite are 2.98 g/cm³ [20] and 2.92 g/cm³ (calculated by the Appen's method [21]), respectively. The difference is more pronounced in the case of diopside, since it is much denser in the crystalline state (3.27 g/cm³) than in glassy phase (2.75 g/cm³). Accordingly, if crystallization proceeds beyond a certain limit, then the occurrence of volume changes results in the development of new pores (defined as secondary porosity) and the enlargement of the existing ones [1]. In this study, the slight reduction of density of the samples heat treated at 800 °C, comparing to values obtained after heat treatment at 700–750 °C (Fig. 3), should be

Table 2

Flexural strength (in MPa) of glass-powder compacts sintered at different temperatures for 1 h

Sample	Temperature (°C)		
	700	750	800
A	92.61 ± 6.8	96.40 ± 6.52	92.95 ± 17.95
A-P	83.63 ± 13.15	109.45 ± 15.10	109.21 ± 4.21

Table 3

Properties of glass-ceramics made of glass-powder compacts sintered at 800 °C for 1 h

Properties	A	A-P
Colour	White	White
Density (g/cm ³)	2.77	2.86
Linear shrinkage (%)	12.6	13.6
Vickers microhardness (GPa)	4.01 ± 0.20	4.43 ± 0.66
Flexural strength (MPa)	93 ± 18	109 ± 4
Coefficient of thermal expansion (10 ⁻⁶ K ⁻¹)		
70–500 °C	9.35	9.90
70–750 °C	9.78	10.20
Water absorption (%)	0.26	0.16

attributed to the effect of secondary porosity, which was more pronounced over heat treatment at higher temperatures (>800 °C).

Table 2 summarizes the bending strength values of the investigated glass-ceramics sintered at 700, 750 and 800 °C for 1 h. In the case of A composition, there is a negligible influence of sintering temperature on flexural strength within the investigated temperature range. In the case of A-P, the maximum strength was obtained after sintering at 750 °C while there was no change over sintering up to 800 °C.

The properties of the investigated glass-ceramics obtained after heat treatment at 800 °C for 1 h are listed in the Table 3. Owing to the fact of the low temperature of heat treatment, the overall evaluation of the values of all the properties measured in this work supports the conclusion that the produced sintered materials possess very good properties. Many glass-ceramics produced by bulk nucleation and crystallization or by sintering of glass-ceramics exhibit similar characteristics but after heat treatment at considerably higher temperatures [4,22,23].

4. Conclusions

The bulk-glasses of composition A and the P_2O_5 -doped composition A-P are prone to surface crystallization and the resultant glass-ceramics have a non-homogeneous crystalline microstructure which comprises relatively coarse crystals.

Glass-ceramics were successfully synthesized via sintering and crystallization of glass-powder compacts. Sintering stage almost ends before the beginning of intensive crystallization. Akermanite predominantly precipitates at ≥700 °C, while weak evidence of formation of diopside was

detected at 750 °C and at 800 °C, slightly stronger in the A-P glass-ceramics.

Doping with P₂O₅ improved the sintering behaviour and broadened the sintering temperature range. The A-P glass-ceramics maintained constant values of the properties over a wide range of sintering temperatures.

Acknowledgements

This work was supported by CICECO and the Portuguese Foundation for Science and Technology.

References

- [1] C. Lira, A.P.N. Oliveira, O.E. Alarcon, Sintering and crystallization of CaO–Al₂O₃–SiO₂ glass powder compacts, *Glass Technol.* 42 (2001) 91–96.
- [2] S.H. Knickerbocker, A.H. Kumar, L.W. Herron, Cordierite glass-ceramics for multilayer ceramic packaging, *Am. Ceram. Soc. Bull.* 72 (1993) 90–95.
- [3] C.L. Lo, J.G. Duh, B.S. Chiou, W.H. Lee, Low temperature sintering and microwave dielectric properties of anorthite based glass-ceramic, *J. Am. Ceram. Soc.* 85 (2002) 2230–2235.
- [4] W. Höland, G. Beall, *Glass-Ceramic Technology*, The American Ceramic Society, Westerville, Ohio, 2002, pp. 287–309.
- [5] T. Toya, Y. Tamura, Y. Kameshima, K. Okada, Preparation and properties of CaO–MgO–Al₂O₃–SiO₂ glass-ceramics from kaolin clay refining waste (Kira) and dolomite, *Ceram. Int.* 30 (2004) 983–989.
- [6] T. Toya, Y. Mameshima, A. Yasumori, K. Okada, Preparation and properties of glass-ceramic clay wastes (kira) of silica and kaolin clay refining, *J. Eur. Ceram. Soc.* 24 (2004) 2367–2372.
- [7] L. Barbieri, A.C. Bonamartini, A.C. Lancellotti, Alkaline and alkaline earth silicate glasses and glass-ceramics from municipal and industrial wastes, *J. Eur. Ceram. Soc.* 20 (2000) 2477–2483.
- [8] A.V. Gorokhovskiy, J.I.E. Garsia, Inorganic wastes in manufacturing of glass and glass-ceramics: quartz-feldspar waste of ore refining, metallurgical slag and limestone, *J. Am. Ceram. Soc.* 85 (2002) 285–287.
- [9] C. Siligardi, M.C. D'Arrigo, C. Lionelli, Sintering behaviour of glass-ceramic frits, *Am. Ceram. Soc. Bull.* 79 (2000) 88–93.
- [10] R.M. German, *Powder Metallurgy Science*, second ed., Metal Powder Industries Federation, New Jersey, 1994, pp. 268–269.
- [11] F.J. Torres, J. Alarcon, Mechanism of crystallization of pyroxene-based glass-ceramic glazes, *J. Non-Cryst. Sol.* 34 (2004) 45–51.
- [12] A.A. Omar, S.M. Salman, M.Y. Mahmoud, Phase relations in the diopside-anorthite-akermanite system, *Ceram. Int.* 12 (1986) 53–59.
- [13] S.N. Salama, H. Darwish, H.A. Abo-Mosallam, Crystallization and properties of glasses based on diopside–Ca–Tschermak's-fluorapatite system, *J. Eur. Ceram. Soc.* 25 (7) (2005) 1133–1142.
- [14] C.K. Chang, D.L. Mao, J.S. Wu, Characteristic of crystals precipitated in sintered apatite/wollastonite glass ceramics, *Ceram. Int.* 26 (2000) 779–785.
- [15] J.J. Shyu, H.H. Lee, Sintering crystallization and properties of B₂O₃/P₂O₅ doped Li₂O–Al₂O₃·4SiO₂ glass-ceramics, *J. Am. Ceram. Soc.* 78 (1995) 2161–2167.
- [16] D.U. Tulyaganov, A.A. Ismatov, Development and application of anorthite-diopside containing glass-ceramics, *Ceram. Trans.* 29 (1993) 221–224.
- [17] D.M. Miller, Sintered cordierite glass-ceramic bodies, USA Patent 3.926.648, 29 May (1976).
- [18] I.W. Donald, B.L. Metcalfe, S.K. Fong, The influence of B₂O₃ additions on the thermal properties and crystallization kinetics of a sodium aluminium phosphate glass, in: *Proceedings of the XX International Congress on Glass*, 26 September–1 October, Kyoto, Japan, 2004.
- [19] A. Karamanov, M. Pelino, A. Hreglich, Sintered glass-ceramics from municipal solid waste incinerator fly ashes, part I: The influence of the heating rate on the sinter crystallization, *J. Eur. Ceram. Soc.* 23 (2003) 817–832.
- [20] JCPDS card of akermanite-synthetic No 87-0052.
- [21] A.A. Appen, *The Chemistry of Glasses*, Himiq, Leningrad, 1974, in Russian.
- [22] Z. Strnad, *Glass-Ceramic Materials*, Elsevier, Amsterdam, 1986.
- [23] A. Karamanov, L. Arriza, I. Matekovits, M. Pelino, Properties of sintered glass-ceramics in the diopside-albite system, *Ceram. Int.* 30 (2004) 2119–2135.